Radially Aligned, Electrospun Nanofibers as Dural Substitutes for Wound Closure and Tissue Regeneration Applications

Jingwei Xie,[†,⊥] Matthew R. MacEwan,[†,⊥] Wilson Z. Ray,[‡] Wenying Liu,[§] Daku Y. Siewe,[†] and Younan Xia[†,*]

[†]Department of Biomedical Engineering, Washington University, St. Louis, Missouri 63130, [‡]Department of Neurosurgery, Washington University, School of Medicine, St. Louis, Missouri 63110, and [§]Department of Energy, Environmental & Chemical Engineering, Washington University, St. Louis, Missouri 63130. [⊥]These authors contributed equally to this work.

ABSTRACT This paper reports the fabrication of scaffolds consisting of radially aligned poly(ε-caprolactone) nanofibers by utilizing a collector composed of a central point electrode and a peripheral ring electrode. This novel class of scaffolds was able to present nanoscale topographic cues to cultured cells, directing and enhancing their migration from the periphery to the center. We also established that such scaffolds could induce faster cellular migration and population than nonwoven mats consisting of random nanofibers. Dural fibroblast cells cultured on these two types of scaffolds were found to express type I collagen, the main extracellular matrix component in dural mater. The type I collagen exhibited a high degree of organization on the scaffolds of radially aligned fibers and a haphazard distribution on the scaffolds of random fibers. Taken together, the scaffolds based on radially aligned, electrospun nanofibers show great potential as artificial dural substitutes and may be particularly useful as biomedical patches or grafts to induce wound closure and/or tissue regeneration.

KEYWORDS: electrospinning · aligned nanofibers · dural substitutes · wound closure

Dura mater is a membranous connective tissue located at the outermost of the three layers of the meninges surrounding the brain and spinal cord, which covers and supports the dural sinuses and carries blood from the brain toward the heart.[1] Dural substitutes are often needed after a neurosurgical procedure to expand or replace the resected dura mater.[2] Although many efforts have been made, the challenge to develop a suitable dural substitute has been met with limited success.[3] Autografts (*e.g.*, fascia lata, temporalis fascia, and pericranium) are preferred because they do not provoke severe inflammatory or immunologic reactions, but they are limited by potential drawbacks such as difficulty in achieving a watertight closure, formation of scar tissue, insufficiently accessible graft materials to close large dural defects, and additional incisions for harvesting the graft.[4,5] Allografts and xenografts are often associated with adverse effects such as graft dissolution, encapsulation, foreign body reaction, scarring, and adhesion formation. Lyophilized human dura mater as a dural substitute has also been clarified as a source of Creutzfeldt-Jakob disease.[6,7]

In terms of materials, nonabsorbable synthetic polymers, such as silicone and expanded polytetrafluoroethylene (ePTFE), often cause serious complications. These may include induction of granulation tissue formation due to their chronic stimulation of the surrounding tissues and long-term foreign body reactions.[8−10] Natural absorbable polymers, including collagen, fibrin, and cellulose, present the potential risk of infection.[11] As a result, synthetic polymers such as poly(3-hydroxybutyrate-*co*-3-hydroxyvalerate) (PHBV), poly(lactic acid) (PLA), polyglycolic acid (PGA), PLA-PCL-PGA ternary copolymers, and hydroxyethylmethacrylate hydrogels have recently attracted attention as biodegradable implant materials for dural repair.[3,5,8−11] Because of their bioabsorbability, they are expected to cause only a small risk of infection with some minor long-term adverse effects. In order to facilitate successful regeneration/repair of the dura mater following surgery, the synthetic dural substitute or patch must promote (*i*) adhesion of dural fibroblasts (the primary cell type present in the dura) and (*ii*) migration of dural fibroblasts from the periphery of the substitute toward the center. So far, synthetic dural substitutes have only been tested in the form of foils, films, meshes, glues, and hydrogels.[12−14] Due to their isotropic surface properties, such substitutes are not well-suited for cell attachment and inward migration. This problem can be potentially solved by processing the polymers as nanoscale fibers with a right alignment. One recent study demonstrated that the speed of cell

*Address correspondence to xia@biomed.wustl.edu.

Received for review July 7, 2010 and accepted August 02, 2010.

Published online August 9, 2010. 10.1021/nn101554u

migration tended to decrease with increasing incubation time on a flat surface, whereas cells could migrate over a relatively long distance with a constant velocity and in a highly correlated fashion on a uniaxially aligned, fibrous scaffold.[15]

Electrospinning is an enabling technique which can produce nanoscale fibers from more than 100 different polymers.[16] The electrospun nanofibers are typically collected as nonwoven mats with random orientation. Uniaxially aligned arrays of nanofibers can also be obtained under certain conditions such as use of an air-gap collector or a mandrel rotating at a high speed.[17,18] However, uniaxially aligned nanofiber scaffolds can only promote cell migration along one specific direction and are thus not useful as dural substitutes. In order to promote cell migration from the surrounding tissue to the center of a dural defect and shorten the time for healing and regeneration of dura mater, a surface patterned with a radially aligned, nanoscale features would be highly desired for an artificial dural substitute. More specifically, scaffolds constructed with radially aligned nanofibers could meet such a demand by guiding and enhancing cell migration from the edge of a dural defect to the center. As compared to other techniques (*e.g.*, photolithography, e-beam writing, and jet printing) capable of generating nanoscale features, electrospinning technique is advantageous in the following aspects: (*i*) electrospun nanofibers are more physiologically relevant as they can mimic the 3D architecture of the extracellular matrix; (*ii*) electrospinning is simpler, faster, and lower in cost for generating patterned nanoscale features such as the radially aligned array of nanofibers used in the present work; and (*iii*) there is essentially no limitation to the materials that can be used for electrospinning. In the present work, we chose poly(ε-caprolactone) (PCL), an FDA approved, semicrystalline polyester that can degrade *via* hydrolysis of its ester linkages under physiological conditions with nontoxic degradation products, as the electrospun polymer for dura substitutes. This polymer has been used in the human body as a material for fabrication of drug delivery carriers, sutures, and adhesion barriers.[19,20] Electrospun PCL nanofibers have also been investigated as scaffolds for a wide variety of applications in tissue engineering.[21−24] Here we demonstrate, for the first time, that electrospun PCL nanofibers can be aligned radially to generate scaffolds potentially useful as dural substitutes.

RESULTS AND DISCUSSION

Figure 1A shows a schematic of the electrospinning setup which consists of a high-voltage generator, a syringe pump, and a collector. It is essentially the same as the conventional setup except for the collector, which includes a metallic ring (the ring electrode) and a metallic needle (the point electrode). Neglecting the effect of charges on the fibers, the electrical potential field can be calculated using the Poisson equation, $\nabla^2 V = -\rho/\varepsilon$, where V is the electrical potential, ε is the electrical permittivity of air, and ρ is the density of space charges. The electrical field, E, can then be calculated by taking the negative gradient of the electrical potential field, $E = -\nabla V$. Here, the electrical field was calculated using the software COMSOL3.3 to verify the alignment effect. Figure 1B shows a 2D cross-sectional view of the electric field strength vectors between the spinneret and the grounded collector. Unlike the conventional system, the electric field vectors (stream lines) in the vicinity of the collector were split into two fractions, pointing toward both the ring and point electrodes. Figure 1C shows a photograph of a typical scaffold consisting of radially aligned electrospun nanofibers that were directly deposited on the collector. Figure 1D shows an SEM image taken from the same scaffold, confirming that the nanofibers had been aligned in a radial fashion.

Dura mater is a complex, fibrous membrane that consists of numerous cells and cell types, extracellular matrix proteins, and trophic factors, all of which play important roles in the colonization and duralization of artificial dural substitutes and thus successful implementation of such grafts *in vivo*. In order to evaluate the capability of radially aligned nanofibers to interface with natural dura, promote host cell adhesion to the graft, and enhance host cell migration along the graft, we developed an *ex vivo* model for the surgical repair of a small dural defect. In a typical procedure, an artificial dural defect was introduced into a piece of dura (1 cm $\times$ 1 cm) by microsurgically cutting a small circular hole 7 mm in diameter in the center of the specimen. A nanofiber-based scaffold was then utilized to repair the artificial defect by overlaying the graft onto the dural specimen. The graft covered the entire defect while simultaneously contacting the dural tissue at the periphery of the specimen. Figure S1 (Supporting Information) shows a schematic illustration of a dural tissue seeded on the edge of a scaffold. As shown in Figure 2A, dural fibroblasts stained with fluorescein diacetate (FDA) migrated from the surrounding tissue along the radially aligned nanofibers and further to the center of the circular scaffold after incubation for 4 days. We found that the cells could cover the entire surface of the scaffold in 4 days. In contrast, a void was observed after the same period of incubation time for a scaffold made of random fibers (Figure 2B), indicating a faster migration rate for the cell on radially aligned nanofibers than on their random counterparts. Figure 2C,D shows magnified views of the central regions in Figure 2A,B, respectively. It is clear that the scaffold made of radially aligned nanofibers was completely populated with dural cells which had migrated from the borders of the apposed dural tissue. On the contrary, we can clearly see the acellular region at the center of the scaffold

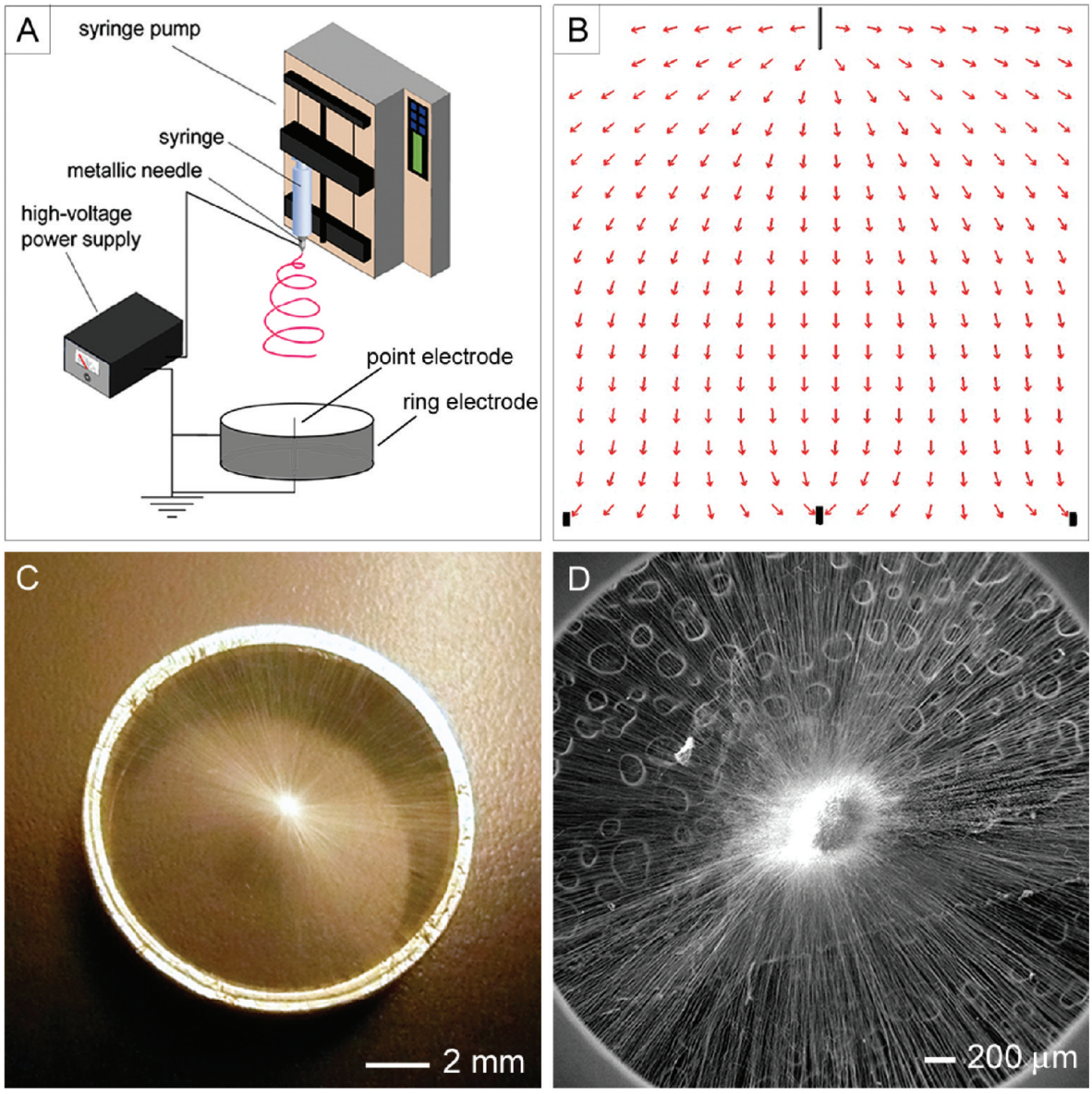

Figure 1. (A) Electrospinning setup for generating scaffolds consisting of radially aligned nanofibers. (B) Electric field strength vectors calculated for the region between the spinneret and the collector. (C) Photograph of a scaffold of radially aligned nanofibers directly deposited on the ring collector. (D) SEM image showing the radial alignment for the nanofibers in the scaffold. The circular features behind the nanofibers were dents on the conductive carbon tape.

made of random nanofibers after the same incubation time.

In order to further investigate the effect of fiber alignment and surface coating on cell migration, primary dural fibroblasts isolated from dura tissue were cultured on scaffolds of radially aligned and random nanofibers without and with fibronectin coating. Figure S2 (Supporting Information) shows a schematic of the custom-made culture system. Specifically, dural fibroblasts were selectively seeded around the periphery of a circular scaffold of nanofibers, effectively forming a 7 mm simulated dural defect in the center of the sample. The silicone tube was used as a barrier to keep the cells in the ring-shaped area during the first 4 h after cell seeding, and then it was removed. Figure 3 shows cell morphology and distribution on scaffolds of radially aligned and random nanofibers without and with fibronectin coating after incubation for 1 day. As shown in Figure 3A, many cells could attach to the bare scaffold of radially aligned nanofibers. In comparison, fewer cells attached to the bare scaffold of random nanofibers and cell aggregations were noticed (Figure 3B). The cells were distributed evenly over the entire surface of the fibronectin-coated scaffold of radially aligned nanofibers, and they exhibited an elongated shape (Figure 3C). This result indicates that fibronectin coating could enhance the influence of topographic cues on cell morphology that were rendered by the alignment of fibers. The cells could also adhere well to the fibronectin-coated scaffold consisting of random nanofibers, and cell distribution was more uniform than the uncoated sample (Figure 3D).

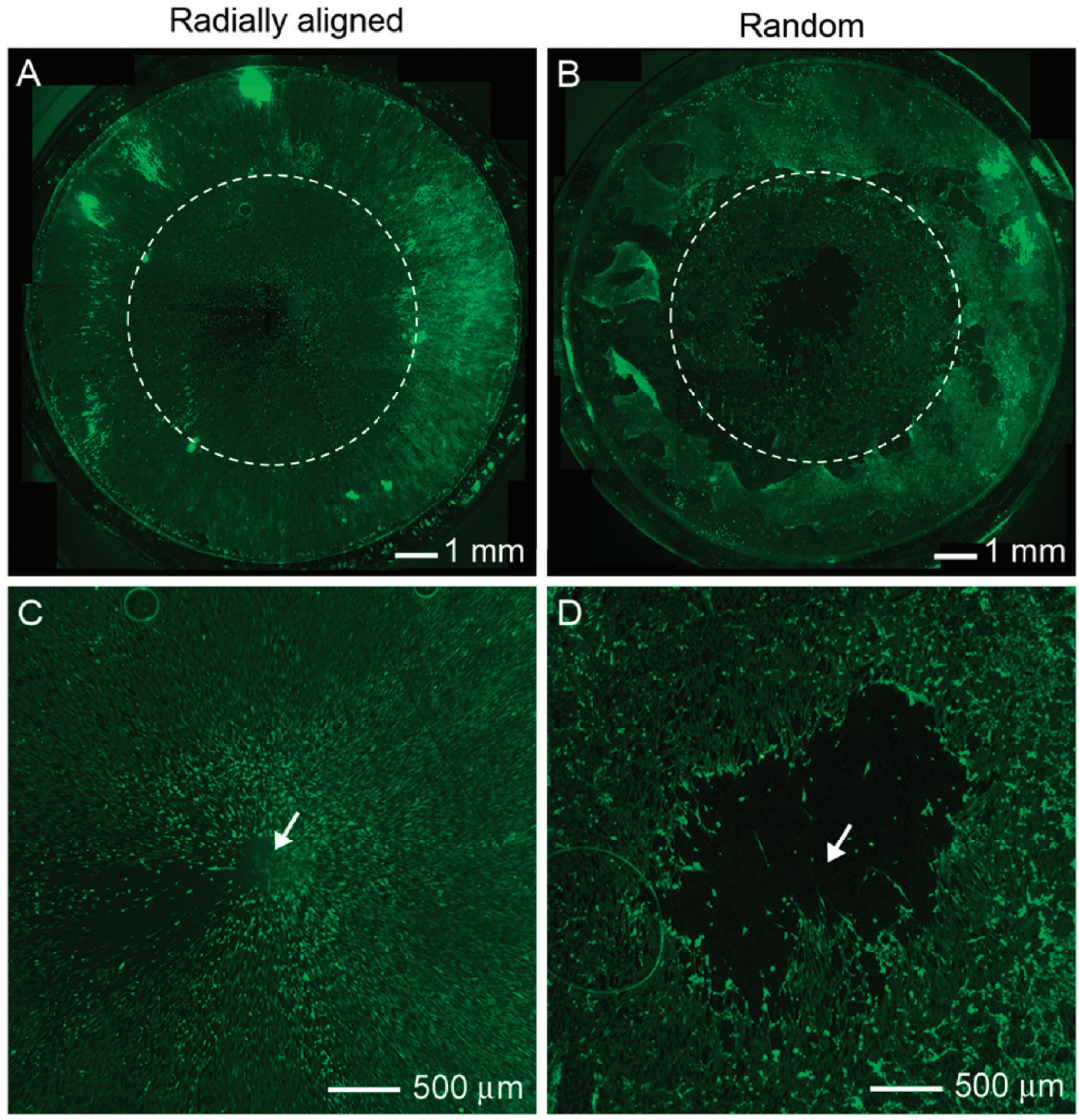

Figure 2. (A,B) Fluorescence micrographs comparing the migration of cells when dura tissues were cultured on scaffolds of radially aligned and random nanofibers, respectively, for 4 days. The dashed circle line indicates the border of dura cells after seeding at day 0. (C,D) Magnified views of the center portion shown in (A) and (B), respectively. The arrow marks the center of the scaffold. In (A), the non-uniformity in cell distribution was probably caused by the slight difference in nanofiber density.

To characterize cell motility on the scaffold, cells were stained with FDA and fluorescence images were taken at different times. Figure 4A−C shows cell distribution after seeding on fibronectin-coated scaffolds of radially aligned nanofibers on days 1, 3, and 7 of culture. The cells were radially aligned, replicating the alignment of fibers underneath (see Figure 4D for a blow-up). The ability for dural fibroblasts to migrate into and repopulate the simulated dural defect was measured at various times throughout the experiment as an estimate of the regenerative capacity of the substitute. Figure 4E illustrates an example for the calculation of the area of simulated dural defect on the scaffold. The area of void was quantified, as shown in Figure 4F. The area of void decreased with increasing incubation time for all the scaffolds we tested due to the inward migration of cells. Obviously, radially aligned fibers could significantly enhance cell migration when compared to random fibers, and cells had the fastest migration rate on the fibronectin-coated scaffold of radially aligned nanofibers for the first 3 days of incubation. We noticed that about 5 mm^2 of bare surface still remained for the bare scaffold of random scaffolds even after incubation for 7 days. In contrast, cells almost covered the entire area of the simulated defect within the same period of incubation time for the other three types of scaffolds. The cell motility toward the center of a fibronectin-coated scaffold of radially aligned nanofibers with increasing incubation time was further confirmed by time lapse imaging shown in Figures S3 and S4 (Supporting Information).

We also compared the scaffolds consisting of radially aligned nanofibers with DuraMatrix-Onlay collagen dura substitute membranes (the clinical gold standard)

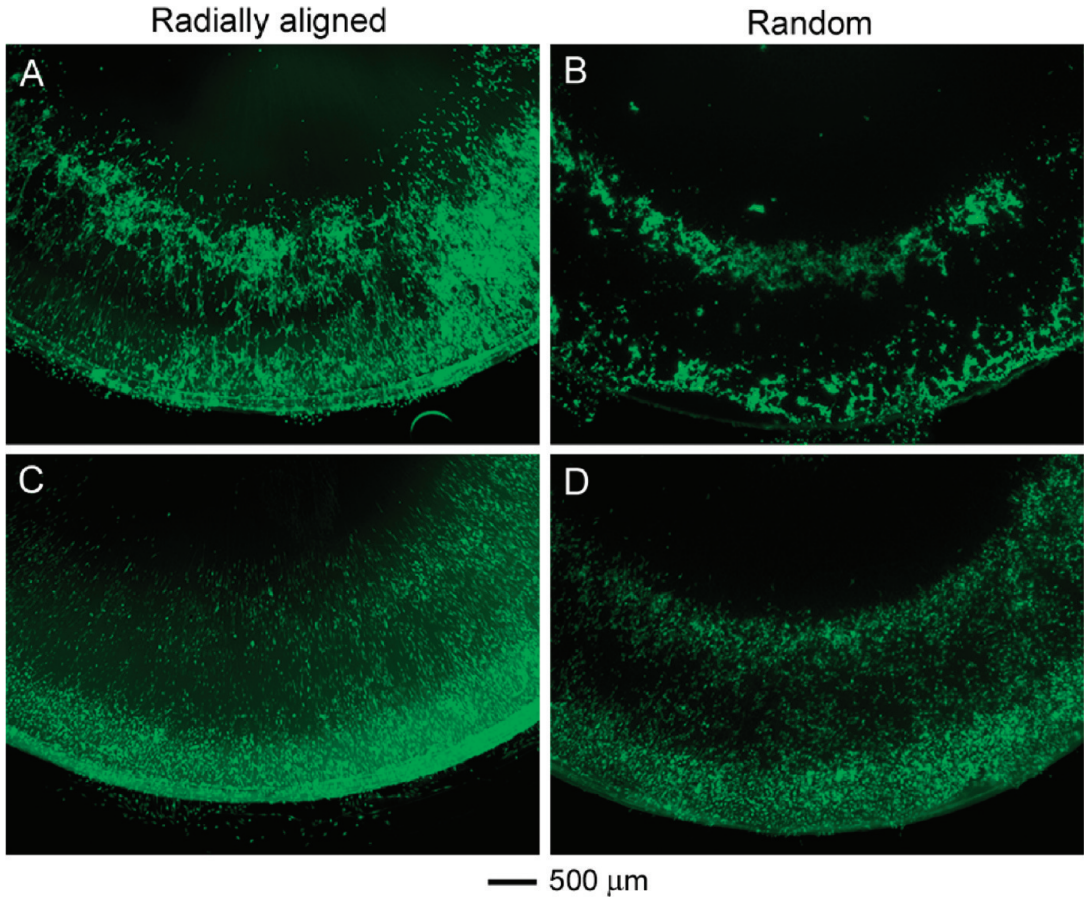

Figure 3. Fluorescence micrographs showing the migration of dura fibroblasts seeded on four different types of nanofiber-based scaffolds for 1 day: (A) radially aligned and bare; (B) random and bare; (C) radially aligned with fibronectin coating; and (D) random with fibronectin coating.

by assessing the attachment and migration of dural fibroblasts. In order to achieve this goal, we seeded dura fibroblasts in the surrounding areas of these two types of scaffolds for 7 days and then stained with FDA. Figure 5A shows cell distribution on a scaffold of radially aligned nanofibers, showing that many cells migrated from the peripheral region to the center of the scaffold and populated throughout the scaffold. Figure 5B shows a high magnification image, indicating that the cells were elongated and aligned along the long axes of fibers. In contrast, we only saw sparse cells on the collagen dura substitute membrane (Figure 5C). The background fluorescence was due to the strong absorption of FDA by the collagen dura substitute membrane. In addition, we noticed that some of the cells appeared round in shape, indicating that the cells seemed to attach and spread poorly on the collagen dura substitute (Figure 5D and Figure S5a in Supporting Information). As shown by the SEM image in Figure S5b, the collagen dura substitute membranes were made of random collagen nanofibers.

Dural tissue is primarily composed of type I collagen.[13,25,26] We also examined the production of type I collagen from dural fibroblasts. Figure 6 shows immunostaining of type I collagen produced by dural fibroblasts which were seeded on various types of nanofiber-based scaffolds. We observed that comparable levels of type I collagen were produced by cells on the scaffolds of radially aligned fibers as compared to those on the scaffolds of random fibers, although one previous study showed that more elongated cells expressed higher collagen type I than less stretched cells.[27] Additionally, fibronectin coating had no significant influence on the production of type I collagen. The type I collagen was oriented haphazardly for the random scaffolds and showed a high degree of organization for the radially aligned scaffolds.

Recent advances in cell−biomaterials interaction have shown that both chemical and topographical properties of the materials' surface can regulate and control cell shape and function.[28] Cell orientation, motility, adhesion, and shape can be modulated by a specific surface micro- and nanotopography. It is well-known that cells can align along microgrooves or similar topographical features on a surface. It was demonstrated that fibroblasts were the most sensitive cell type compared to endothelial cells and smooth muscle cells and often responded with a strong alignment, elongation, and migration along the grooves.[29] Simultaneously, electrospinning has been widely used for pro-

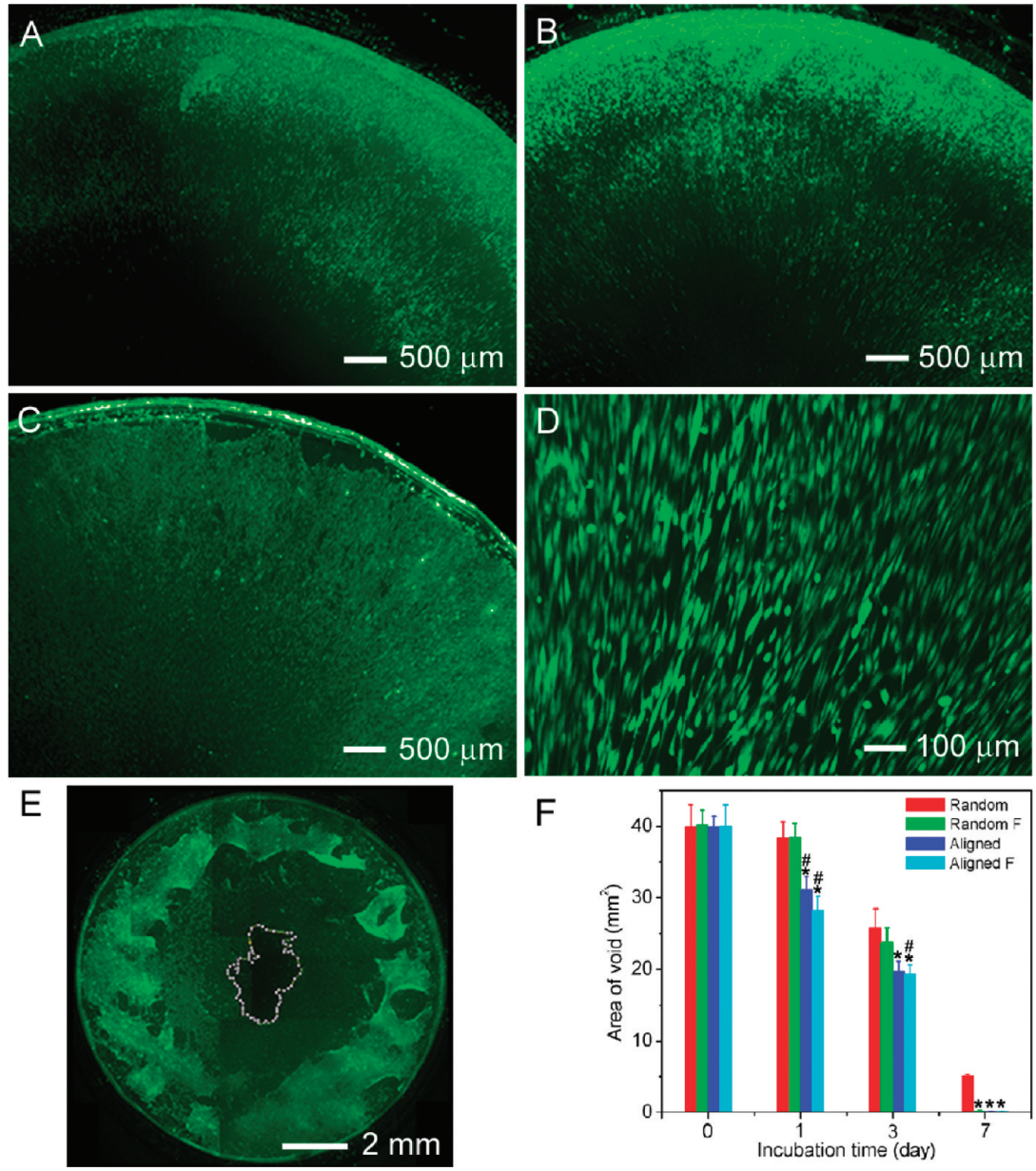

Figure 4. Fluorescence micrographs showing the migration of dura fibroblasts seeded on fibronectin-coated scaffolds of radially aligned nanofibers for (A) 1 day, (B) 3 days, and (C) 7 days. (D) Higher magnification view of the sample in (C). (E) Illustration showing how to calculate the area of void space. (F) Area of void space as a function of incubation time; ∗ and # indicate $p < 0.05$ for samples compared with random samples and random F samples in the same period of incubation time. Random: scaffold of random fibers. Random F: fibronectin-coated scaffold of random fibers. Aligned: scaffold of radially aligned fiber. Aligned F: fibronectin-coated scaffold of radially aligned fibers.

ducing nanofibers for a rich variety of applications in tissue engineering including skin grafts, artificial blood vessels, nerve conduits, along with others.[30−32] Yet, previous studies were limited to the use of scaffolds made of random and uniaxially aligned nanofibers. Although it was demonstrated that cells migrated faster on uniaxially aligned nanofibers than random fibers,[33] scaffolds composed of uniaxially aligned nanofibers were not realistic for wound healing applications due to the irregular shape of the wound. In the present work, we demonstrated for the first time the fabrication of a new type of scaffolds consisting of radially aligned nanofibers. This novel type of scaffold can guide dural fibroblasts spreading along the direction of fiber alignment and direct cell motility toward the center of the scaffold, resulting in faster cell migration compared to scaffolds composed of random nanofibers. In addition, uniaxially aligned nanofiber scaffolds cannot match such a capability in that they can only guide cell migration along one specific direction. It was reported that controlling cellular orientation or morphology by topography or so-called "contact guidance" could allow for the organization of the extracellular matrix.[34−36] For most injuries, natural healing results in once functional tissue becoming a scar which is usually made of a patch of cells (*e.g.*, fibroblasts) and disorganized extracellular matrix

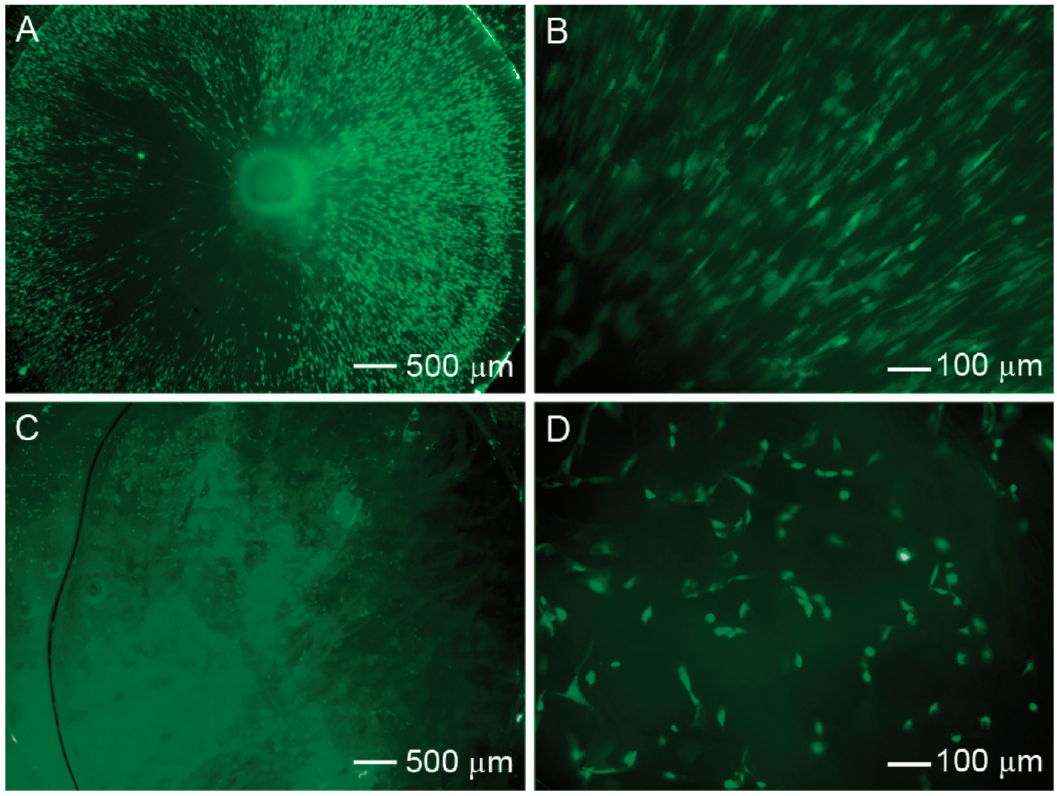

Figure 5. Fluorescence micrographs showing dura fibroblasts migrated from peripheral region toward the center for 7 days on (A,B) fibronectin-coated scaffolds of radially aligned nanofibers and (C,D) DuraMatrix-Onlay collagen dura substitute membrane. In (A), the non-uniformity in cell distribution was probably caused by the slight difference in nanofiber density.

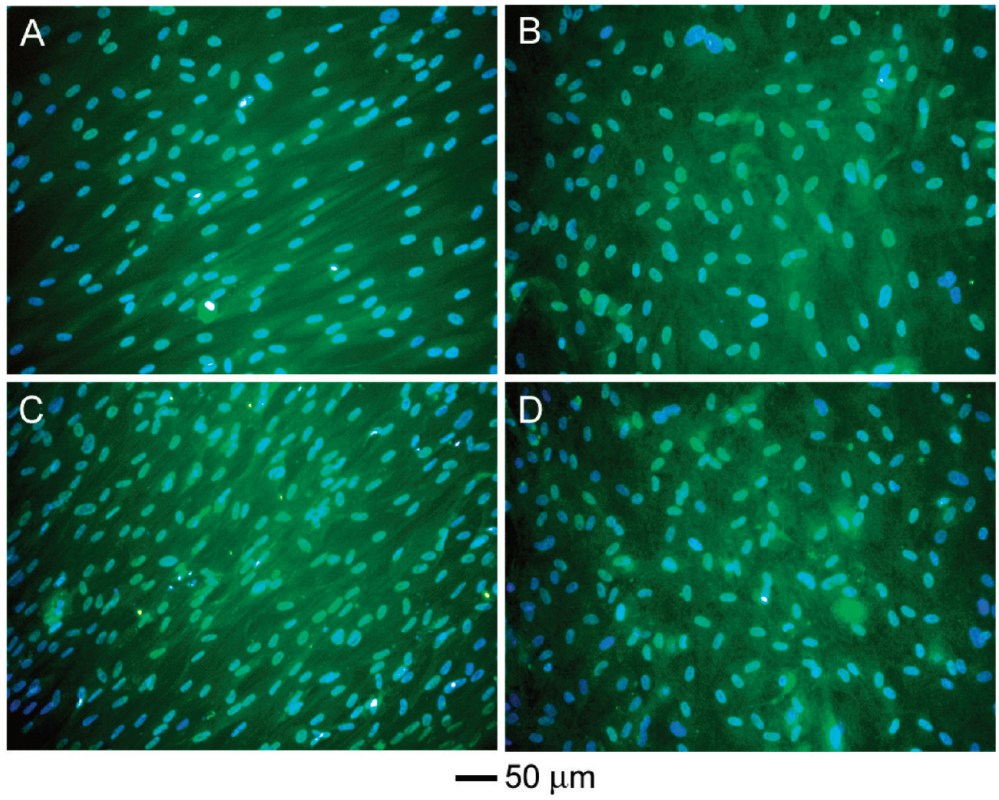

Figure 6. Fluorescence micrographs obtained by immunostaining with monoclonal antibodies for type I collagen in green and DAPI for cell nuclei in blue for the scaffolds consisting of (A,C) radially aligned and (B,D) random fibers, respectively. The scaffolds in (A,B) were not coated with fibronectin while those in (C,D) were.

(*e.g.*, collagen fibers).[37] Highly organized cells and an extracellular matrix are probably required for tissue regeneration, which is normally not thought to be related to tissue repair with scarring. We have demonstrated in the present work that extracellular matrix type I collagen on scaffolds of radially aligned nanofibers showed a high degree of organization, which may reduce the possibility of scar tissue formation.

The ideal dura substitute should be safe, efficacious, easy to handle, watertight and integrated into the surrounding tissue to form a new tissue similar to the native one.[2] Also, it should avoid harmful foreign body reactions, be free of any potential risk of infections, have mechanical properties similar to those of natural dura mater, in particular with respect to flexibility and strength, be storable and readily available when needed.[3,12,13] In the present work, the biodegradable polymer PCL was chosen as a material for dural substitute because PCL has some advantages compared with other bioabsorbable polyesters. Heterogeneous degradation of PGA and poly(L-lactic acid) (PLLA) could lead to a sudden increase of degradation products, resulting in acidic conditions and toxic reactions in the surrounding tissue.[3] The degradation of PCL is slower, produces less acidic degradation products, and has been studied as a wound dressing material since the 1970s.[38] In order to obtain watertight property, the radially aligned nanofiber scaffold can be combined with a nonwoven mat to form two-layered or even multilayered substitutes. Simultaneously, antibiotics can be readily encapsulated inside nanofibers to further reduce inflammatory response, improve wound healing, and prevent postsurgery adhesion.[39,40] Alternatively, PCL can blend with other polymers to further improve its biocompatibility, as well as mechanical, physical, and chemical properties.[38] Moreover, extracellular proteins and/or growth factors can be immobilized on the surface of the nanofibers using various surface modification approaches to enhance cell adhesion. The current work presented the effect of fibronectin coating on the PCL nanofibers through electrostatic interaction on dural fibroblast adhesion and motility. One previous study reported that basic fibroblast growth factor (bFGF) immobilized on electrospun PLA nanofibers had less effect on skin cell migration.[33] Our results demonstrated that fibronectin coating enhanced adhesion of dural fibroblasts and improved cell migration on randomly oriented nanofiber scaffolds, but the coating had marginal contribution to cell motility on radially aligned nanofiber scaffolds compared to the bare scaffolds, indicating the predominant role played by nanofiber alignment.

CONCLUSIONS

In summary, we have demonstrated the fabrication of a new type of electrospun nanofiber scaffold composed of radially aligned fibers and its potential application as dural substitutes. We showed that dural fibroblasts cultured on scaffolds of radially aligned nanofibers were elongated and their migration toward the center of the scaffold was greatly accelerated along with the development of a regular arrangement of extracellular matrix like type I collagen, potentially allowing for fast regeneration and formation of neodura. Taken together, our results suggest that radially aligned nanofibers as an artificial dural substitute may offer an alternative in the repair of dural defects and furthermore occupy a unique, desirable niche within the neurosurgical community.

EXPERIMENTAL METHODS

Fabrication of Electrospun Nanofiber Scaffolds. In a typical procedure for electrospinning PCL (M_w = 65 kDa, Sigma-Aldrich) nanofibers, we used a solution of 20% (w/v) PCL in a mixture of dichloromethane (DCM) and *N*,*N*-dimethylformamide (DMF) (Fisher Chemical) with a volume ratio of 4:1. The fibers were spun at 10−17 kV with a feeding rate of 0.5 mL/h, together with a 23 gauge needle as the spinneret. A piece of aluminum foil was used as a collector to obtain random nanofiber scaffolds. Radially aligned nanofiber scaffolds were fabricated utilizing a collector consisting of a ring electrode (*e.g.*, metal ring) and a point electrode (*e.g.*, a sharp needle). Electrospun PCL nanofibers were coated with fibronectin (Millipore, Temecular, CA) as follows. The electrospun fiber scaffolds were sterilized by soaking in 70% ethanol overnight and washed three times with phosphate buffered saline (PBS). Then, the scaffolds were immersed in a 0.1% poly-L-lysine (PLL) (Sigma-Aldrich) solution for 1 h at room temperature, followed by washing with PBS (Invitrogen) three times. Subsequently, the samples were immersed in a fibronectin solution (26 μL of 50 μg/mL fibronectin solution diluted with 5 mL of PBS buffer) at 4 °C overnight. Prior to cell seeding, the fibronectin solution was removed and the nanofiber scaffolds were rinsed with PBS. The DuraMatrix-Onlay collagen dura substitute membrane was kindly provided as a gift from Stryker Craniomaxillofacial (Kalamazoo, MI).

Characterization of Nanofiber Scaffolds. The PCL nanofiber scaffolds were sputter-coated with gold before imaging with a scanning electron microscope (Nova 200 NanoLab, FEI, Oregon, USA) at an accelerating voltage of 15 kV. Samples prepared for use in cell culture were inserted into a 24-well TCPS culture plate and sterilized by soaking scaffolds in 70% ethanol.

Dural Fibroblast Isolation and Culture. Fibroblasts were isolated from sections of dura explanted from 4.5 kg New Zealand rabbits (Myrtle's Rabbitry, Thompsons Station, TN). Dura was obtained from recently euthanized animals through a complete craniotomy performed under sterile conditions. Specifically, a 5.0 cm midline incision was made in the scalp to expose the underlying calvarium. Following periosteal elevation, a 2.5 cm × 3.0 cm section of bone was removed from the calvarium to expose the underlying dura. A 2.0 cm × 1.5 cm section of dura was then removed through sharp dissection and washed three times with cold PBS. Dural fibroblasts were then isolated by digesting minced dura three times in 4 mL of warm Hank's balanced salt solution (HBSS) containing 0.05% Trypsin and 0.04% EDTA (Sigma-Aldrich, St. Louis, MO). Following digestion, collected supernatant was centrifuged and the pellet of dural cells was isolated and resuspended in Dulbecco's modified Eagle's medium (DMEM) supplemented with 10% calf serum and 1% penicillin and streptomycin. Dural cells obtained in this manner were then

plated in 75 cm^2 flasks and expanded (subpassaged no more than five times).

Dural Fibroblast Migration. Large, continuous pieces of dura mater were placed in cold PBS and microsurgically trimmed into 1 cm × 1 cm sections. An artificial defect was then introduced into each section of dura by microsurgically cutting a small circular hole, 7 mm in diameter, in the middle of the section. Sections of dura were then introduced into individual wells of 6-well culture plates containing 4 mL of DMEM supplemented with 10% calf serum and 1% penicillin and streptomycin. Random and radially aligned nanofiber scaffolds 1 cm in diameter were then utilized to repair the artificial defects by overlaying the graft onto the dural specimen. Nanofiber scaffolds were placed on the dura such that the graft covered the entire defect while simultaneously contacting the dural tissue at the periphery of the specimen. Nanofiber scaffolds were held in this position throughout the experiment by placing a sterilized metal ring over both the scaffold and the dura. After 4 days of culture, the cells were stained with FDA in green color and imaged with fluorescence microscope. Fluorescent images were taken using a QICAM Fast Cooled Mono 12-bit camera (Q Imaging, Burnaby, BC, Canada) attached to an Olympus microscope with OCapture 2.90.1 (Olympus, Tokyo, Japan). Similarly, around 1×10^5 dural fibroblast cells were seeded onto the periphery of nanofiber scaffolds using our homemade culture system shown in Figure S2 (Supporting Information). After different periods of time, the cells were stained with FDA in green color and imaged with a fluorescence microscope. The total surface area of nanofiber scaffold devoid of migrating cells was then quantified using Image J software (National Institutes of Health).

Time Lapse Imaging of Dural Fibroblast Migration. Living cells were labeled with membrane dye using Vybrant DiO cell-labeling solution (Invitrogen) according to the manufacturer's instructions and then imaged at day 1, 3, 7, and 10. Dural fibroblasts were seeded on nanofibers and placed on the stage of an optical microscope. The whole setup was placed in the incubator. Cell migration on nanofiber films was imaged every 5 min using Panasonic WV-BP130 attached to a Nikon microscope with FlashBus FBG (Nikon).

Scanning Electron Microscopy Imaging. The dural fibroblast-seeded collagen dura substitute membrane was fixed in 3.7% formaldehyde for 30 min. Subsequently, it was dehydrated in ethanol with a series of concentrations (30, 50, 70, 90, 95, and 100%) and dried in vacuum. Finally, the sample was coated with gold using a sputter prior to imaging by SEM. The accelerating voltage was 15 kV for imaging.

Immunohistochemistry. Production of collagen type I by the dural fibroblasts on the fiber scaffolds was assessed using immunohistochemistry. On day 7, the cells were rinsed with PBS and fixed with 3.7% formalin for 1 h ($N = 4$). Cells were permeabilized using 0.1% Triton X-100 (Invitrogen) in PBS for 20 min, followed by blocking in PBS containing 5% normal goat serum (NGS) for 30 min. The monoclonal antibody for type I collagen (1:20 dilution) was obtained from EMD Chemicals (Calbiochem, San Diego, CA). Cells were washed three times with PBS containing 2% FBS. The secondary antibody Gt × Rb IgG Fluor (Chemicon, Temecula, CA) (1:200 dilution) was applied for 1 h at room temperature. Fluorescent images were taken using a QICAM Fast Cooled Mono 12-bit camera (Q Imaging, Burnaby, BC, Canada) attached to an Olympus microscope with OCapture 2.90.1 (Olympus, Tokyo, Japan).

Statistical Analysis. Mean values and standard deviation were reported. Comparative analyses were performed using the Tukey post hoc test by analysis of variance at a 95% confidence level.

Acknowledgment. This work was supported in part by a 2006 NIH Director's Pioneer Award (DP1 OD000798) and start-up funds from Washington University in St. Louis. Part of the work was performed at the Nano Research Facility (NRF), a member of the National Nanotechnology Infrastructure Network (NNIN), which is supported by the NSF under Award No. ECS-0335765.

Supporting Information Available: Figures S1−S5. This material is available free of charge *via* the Internet at http://pubs.acs.org.

REFERENCES AND NOTES

1. Esposito, F.; Cappabianca, P.; Fusco, M.; Cavallo, L. M.; Bani, G. G.; Biroli, F.; Sparano, A.; Divitiis, O. D.; Signorelli, A. Collagen-Only Biomatrix as a Novel Dural Substitute: Examination of the Efficacy, Safety and Outcome: Clinical Experience on a Series of 208 Patients. *Clin. Neurol. Neurosurg.* **2008**, *110*, 343–351.
2. Gazzeri, R.; Neroni, M.; Alfieri, A.; Galarza, M.; Faiola, A.; Esposito, S.; Giordano, M. Transparent Equine Collagen Biomatrix as Dural Repair. A Prospective Clinical Study. *Acta Neurochir.* **2009**, *151*, 537–543.
3. Bernd, H. E.; Kunze, C.; Freier, T.; Sternberg, K.; Kramer, S.; Behrend, D.; Prall, F.; Donat, M.; Kramp, B. Poly(3-hydroxybutyrate) (PHB) Patches for Covering Anterior Skull Base Defects—An Animal Study with Minpigs. *Acta Oto-Laryngol.* **2009**, *129*, 1010–1017.
4. McCall, T. D.; Fults, D. W.; Schmidt, R. H. Use of Resorbable Collagen Dural Substitutes in the Presence of Cranial and Spinal Infections—Report of 3 Cases. *Surg. Neurol.* **2008**, *70*, 92–97.
5. Shimada, Y.; Hongo, M.; Miyakoshi, N.; Sugawara, T.; Kasukawa, Y.; Ando, S.; Ishikawa, Y.; Itoi, E. Dural Substitute with Polyglycolic Acid Mesh and Fibrin Glue for Dural Repair: Technical Note and Preliminary Results. *J. Orthop. Sci.* **2006**, *11*, 454–458.
6. Yamda, M.; Noguchi-Shinohara, M.; Hamaguchi, T.; Nozaki, I.; Kitamoto, T.; Sato, T.; Nakamura, Y.; Mizusawa, H. Dural Mater Graft-Associated Creutzfeldt-Jakob Disease in Japan: Clinicopathological and Molecular Characterization of the Two Distinct Subtyptes. *Neuropathology* **2009**, *29*, 609–618.
7. Zerris, V. A.; James, K. S.; Roberts, J. B.; Bell, E.; Heilman, C. B. Repair of the Dura Mater with Processed Collagen Devices. *J. Biomed. Mater. Res., Part B* **2007**, *83B*, 580–588.
8. Ohbayashi, N.; Inagawa, T.; Katoh, Y.; Kumano, K.; Nagasako, R.; Hada, H. Complication of Silastic Dural Substitute 20 Years after Dural Plasty. *Surg. Neurol.* **1994**, *41*, 338–341.
9. Chen, J.; Lee, S.; Lui, T.; Yeh, Y.; Chen, T.; Tzaan, W. Teflon Granuloma after Microvascular Decompression for Trigeminal Neuroglia. *Surg. Neurol.* **2000**, *53*, 281–287.
10. Haq, I.; Cruz-Almeida, Y.; Siqueira, E. B.; Norenberg, M.; Green, B. A.; Levi, A. D. CyberKnife Stereotactic Radio Surgical Treatment of Spinal Tumors for Pain Control and Quality of Life. *J. Neurosurg. Spine* **2005**, *2*, 50–54.
11. Mukai, T.; Shirahma, N.; Tominaga, B.; Ohno, K.; Koyama, Y.; Takakuda, K. Development of Watertight and Bioabsorbable Synthetic Dural Substitutes. *Artif. Organs* **2008**, *32*, 473–483.
12. Yamada, K.; Miyamoto, S.; Nagata, I.; Kikuchi, H.; Ikada, Y.; Iwata, H.; Yamamoto, K. Development of a Dural Substitute from Synthetic Bioabsorbable Polymers. *J. Neurosurg.* **1997**, *86*, 1012–1017.
13. Yamada, K.; Miyamoto, S.; Takyama, M.; Nagata, I.; Hashimoto, N.; Ikada, Y.; Kikuchi, H. Clinical Application of a New Bioabsorbable Artificial Dura Mater. *J. Neurosurg.* **2002**, *96*, 731–735.
14. Bhatia, S.; Bergethon, P. R.; Blease, S.; Kemper, T.; Rosiello, A.; Zimbardi, G. P.; Franzblau, C.; Spatz, E. L. A Synthetic Dural Prothesis Constructed from Hydroxyethylmethacrylate Hydrogels. *J. Neurosurg.* **1995**, *83*, 897–902.
15. Liu, Y.; Franco, A.; Huang, L.; Gersappe, D.; Clark, R. A. F.; Rafailovich, M. H. Control of Cell Migration in Two and Three Dimensions Using Substrate Morphology. *Exp. Cell Res.* **2009**, *315*, 2544.
16. Burger, C.; Hsiao, B. S.; Chu, B. Nanofibrous Materials and Their Applications. *Annu. Rev. Mater. Res.* **2006**, *36*, 333–368.
17. Li, D.; Wang, Y.; Xia, Y. Electrospinning of Polymeric and Ceramic Nanofibers as Uniaxially Aligned Arrays. *Nano Lett.* **2003**, *3*, 1167–1171.
18. Li, D.; Xia, Y. Electrospinning of Nanofibers: Reinventing the Wheel. *Adv. Mater.* **2004**, *16*, 1151–1170.

19. Mohan, N.; Nair, P. D. Polyvinyl Alcohol−Poly(caprolactone) Semi IPN Scaffold with Implication for Cartilage Tissue Engineering. *J. Biomed. Mater. Res., Part B* **2008**, *84B*, 584–594.
20. Kweon, H. Y.; Yoo, M. K.; Park, I. K.; Kim, T. H.; Lee, H. C.; Lee, H. S.; Oh, J. S.; Akaike, T.; Cho, C. S. A Novel Degradable Polycaprolactone Networks for Tissue Engineering. *Biomaterials* **2003**, *24*, 801–808.
21. Yoshimoto, H.; Shin, Y. M.; Terai, H.; Vacanti, J. P. A Biodegradable Nanofiber Scaffold by Electrospinning and Its Potential for Bone Tissue Engineering. *Biomaterials* **2003**, *24*, 2077–2082.
22. Reed, C. R.; Han, L.; Andrady, A.; Caballero, M.; Jack, M. C.; Collins, J. B.; Saba, S. C.; Loboa, E. G.; Cairns, B. A.; van Aalst, J. A. Composite Tissue Engineering on Polycaprolactone Nanofiber Scaffolds. *Ann. Plast. Surg.* **2009**, *62*, 505–512.
23. Venugopal, J.; Ramakrishna, S. Biocompatible Nanofiber Matrices for the Engineering of a Dermal Substitute for Skin Regeneration. *Tissue Eng.* **2005**, *11*, 847–854.
24. Li, W. J.; Danielson, K. G.; Alexander, P. G.; Tuan, R. S. Biological Response of Chondrocytes Cultured in Three-Dimensional Nanofibrous Poly(ε-caprolactone) Scaffolds. *J. Biomed. Mater. Res.* **2003**, *67A*, 1105–1114.
25. Dunn, M. G.; Silver, F. H. Viscoelastic Behavior of Human Connective Tissues: Relative Contribution of Viscous and Elastic Components. *Connect. Tissue Res.* **1983**, *12*, 59–70.
26. Cobb, M. A.; Badylak, S. F.; Janas, W.; Simmons-Byrd, A.; Boop, F. A. Porcine Small Intestinal Submucosa as a Dural Substitute. *Surg. Neurol.* **1999**, *51*, 99–104.
27. Li, F.; Li, B.; Wang, Q. M.; Wang, J. H. C. Cell Shape Regulates Collagen Type I Expression in Human Tendon Fibroblasts. *Cell Motil. Cytoskeleton* **2008**, *65*, 332–341.
28. Kulangara, K.; Leong, K. W. Substrate Topography Shapes Cell Function. *Soft Matter* **2009**, *5*, 4072–4076.
29. Biela, S. A.; Su, Y.; Spatz, J. P.; Kemkemer, R. Different Sensitivity of Human Endothelial Cells, Smooth Muscle Cells and Fibroblasts to Topography in the Nano-Micro Range. *Acta Biomater.* **2009**, *5*, 2460–2466.
30. Xie, J.; Li, X.; Xia, Y. Putting Electrospun Nanofibers to Work for Biomedical Research. *Macromol. Rapid Commun.* **2008**, *29*, 1775–1792.
31. Sill, T. J.; Recum, H. A. Electrospinning: Applications in Drug Delivery and Tissue Engineering. *Biomaterials* **2008**, *29*, 1989–2006.
32. Pham, Q. P.; Sharma, U.; Mikos, A. G. Electrospinning of Polymeric Nanofibers for Tissue Engineering Applications. *Tissue Eng.* **2006**, *12*, 1197–1211.
33. Patel, S.; Kurpinski, K.; Quigley, R.; Gao, H.; Hsiao, B. S.; Poo, M. M.; Li, S. Bioactive Nanofibers: Synergistic Effects of Nanotopography and Chemical Signaling on Cell Guidance. *Nano Lett.* **2007**, *7*, 2122–2128.
34. Manwaring, M. E.; Walsh, J. F.; Tresco, P. A. Contact Guidance Induced Organization of Extracellular Matrix. *Biomaterials* **2004**, *25*, 3631–3638.
35. Wang, J. H. C.; Jia, F.; Gilbert, T. W.; Woo, S. L. Y. Cell Orientation Determines the Alignment of Cell-Produced Collagenous Matrix. *J. Biomech.* **2003**, *36*, 97–102.
36. Den Braber, E. T.; de Ruijter, J. E.; Ginsel, L. A.; von Recum, A. F.; Jansen, J. A. Orientation of ECM Protein Deposition, Fibroblast Cytoskeleton, and Attachment Complex Components on Silicone Microgrooved Surfaces. *J. Biomed. Mater. Res.* **1998**, *40*, 291–300.
37. Gurtner, G. C.; Werner, S.; Barrandon, Y.; Longaker, M. T. Wound Repair and Regeneration. *Nature* **2008**, *453*, 314–321.
38. Chong, E. J.; Phan, T. T.; Lim, I. J.; Zhang, Y. Z.; Bay, B. H.; Ramakrishna, S.; Lim, C. T. Evaluation of Electrospun PCL/Gelatin Nanofibrous Scaffold for Wound Healing and Layered Dermal Reconstitution. *Acta Biomater.* **2007**, *3*, 321–330.
39. Bolgen, N.; Vargel, I.; Korkusuz, P.; Menceloglu, Y. Z.; Piskin, E. *In Vivo* Performance of Antibiotic Embedded Electrospun PCL Membranes for Prevention of Abdominal Adhesions. *J. Biomed. Mater. Res., Part B* **2007**, *81B*, 530–543.
40. Zong, X. H.; Li, S.; Chen, E.; Garlick, B.; Kim, K. S.; Fang, D.; Chiu, J.; Zimmerman, T.; Brathwaite, C.; Hsiao, B. S.; Chu, B. Prevention of Postsurgery-Induced Abdominal Adhesions by Electrospun Bioabsorbable Nanofibrous Poly(lactide-*co*-glycolide)-Based Membranes. *Ann. Surg.* **2004**, *240*, 910–915.